

RESEARCH ARTICLE

Open Access



Preliminary comparative analysis of the genomes of selected field reisolates of the *Mycoplasma synoviae* vaccine strain MS-H reveals both stable and unstable mutations after passage in vivo

Somayeh Kordafshari^{*} , Pollob Shil, Marc S. Marenda, Olusola M. Olaogun, Barbara Konsak-Ilievski, Jillian Disint and Amir H. Noormohammadi

Abstract

Background: Genomic comparison of *Mycoplasma synoviae* vaccine strain MS-H and the MS-H parental strain 86, 079/7NS established a preliminary profile of genes related to attenuation of MS-H. In this study we aimed to identify the stability of mutations found in MS-H after passage in experimental or field chickens, and to evaluate if any reverse mutation may be associated with changes in characteristics of MS-H in vitro or in vivo.

Results: Whole genome sequence analysis of 5 selected MS-H field reisolates revealed that out of 32 mutations reported previously in MS-H, 28 remained stable, while four found to be reversible to the wild-type. Each isolate possessed mutations in one to three of the genes *obg*, *oppF₁* and *gap* and/or a non-coding region. Examination of the 4 reversible mutations by protein modeling predicted that only two of them (in *obg* and *oppF₁* genes) could potentially restore the function of the respective protein to that of the wild-type.

Conclusions: These results suggest that the majority of the MS-H mutations are stable after passage in vaccinated chickens. Characterisation of stable mutations found in MS-H could be utilised to develop rapid diagnostic techniques for differentiation of vaccine from field strains or *ts*- MS-H reisolates.

Keywords: *Mycoplasma synoviae*, MS-H vaccine strain, Genomic comparison, Stable and unstable mutations, MS-H field reisolates

Background

Mycoplasma synoviae (MS) is a major poultry pathogen, and due to its high economic impact on sectors of the chicken and turkey industries [1] has been listed as a serious disease of poultry by the World Organization for Animal Health (OIE, <http://www.oie.int/animal-health-in-the-world/oie-listed-diseases-2019/>). Control of the disease

caused by MS through biosecurity and serological monitoring is often insufficient [2]. Therefore, live attenuated vaccines are used when the prevention of exposure is impractical. The most commonly used commercial MS vaccine in Australia (Vaxsafe MS[®]; Bioproperties Ltd., Ringwood, Victoria, Australia) is a temperature sensitive (*ts*+) strain (MS-H) which was developed by chemical mutagenesis of an Australian field isolate 86,079/7NS [3].

A wide range of *ts*+ viruses and bacteria have been used as vaccine candidates, but in many cases it is not

* Correspondence: somayeh.kordafshari@unimelb.edu.au

Asia Pacific Centre for Animal Health, Faculty of Veterinary & Agricultural Sciences, The University of Melbourne, Werribee, Victoria 3030, Australia



© The Author(s). 2020, corrected publication 2020. **Open Access** This article is licensed under a Creative Commons Attribution 4.0 International License, which permits use, sharing, adaptation, distribution and reproduction in any medium or format, as long as you give appropriate credit to the original author(s) and the source, provide a link to the Creative Commons licence, and indicate if changes were made. The images or other third party material in this article are included in the article's Creative Commons licence, unless indicated otherwise in a credit line to the material. If material is not included in the article's Creative Commons licence and your intended use is not permitted by statutory regulation or exceeds the permitted use, you will need to obtain permission directly from the copyright holder. To view a copy of this licence, visit <http://creativecommons.org/licenses/by/4.0/>. The Creative Commons Public Domain Dedication waiver (<http://creativecommons.org/publicdomain/zero/1.0/>) applies to the data made available in this article, unless otherwise stated in a credit line to the data.

exactly known whether temperature sensitivity is the cause of attenuation or just a coincidental phenotype in these organisms [4, 5].

The majority of MS clones recovered from vaccinated flocks display their *ts* + phenotype, but it has been suggested that MS-H proliferation in vaccinated birds generates a mixture of *ts* + and *ts*- clones in the farm [6, 7].

Unlike the non-virulent MSH strain, *ts*- field reisolates cause only minor lesions in the tracheal mucosa of the experimentally infected birds, significantly lower than the vaccine parent strain [7]. These results suggest that factors other than *ts* + phenotype are involved in the attenuation of the MS-H vaccine.

While the genetic basis of the MS-H temperature sensitivity and attenuation is not fully known yet, a mutation detected in *obg* gene was proposed as a likely explanation for the MS-H *ts* + phenotype [8]. Also, further comparison of the MS-H genome with that of its wild-type parent strain 86,079/7NS has revealed a frame-shift mutation in an oligopeptide permease transporter (*opp*) gene, *oppF*₁ [9]. *OppF* is essential in establishment of systemic infection by *M. bovis* and its persistence in lower respiratory tract of calves [10]. Also, *oppD* was found to be required for full expression of virulence of *M. gallisepticum* in chickens [11].

Partial sequence analysis of *obg* and *oppF* genes [8, 12] in five MS-H isolates have found different combinations of *obg* and *oppF* genotypes. Of the five isolates, MS-H³, 101,564 and 101,731 had *obg*^w (w = wild-type) and *oppF*^v (v = vaccine-type), MS-H⁴ had *obg*^w and *oppF*^w, and MS-H⁵ had *obg*^v and *oppF*^w. In this study the MS-H reisolates MS-H³, 101,564, 101,731 MS-H⁴, and MS-H⁵ were subjected to a

comparative genome analysis to establish if any other mutations previously reported for the MS-H [12] may be reversible to the wild-type and evaluate if they could potentially influence MS-H attenuation.

Results

Phylogenetically, all selected reisolates from vaccinated flocks were closely related to MS-H

Illumina paired reads from MS-H field isolates (GenBank accession number PRJNA649354) were De novo assembled successfully using SPAdes with an average 162 of contigs generated for each ranging from 125 to 131,331 bp per isolate. The *vlhA* pseudogene region, a ~50 kb locus covering large number of highly repetitive sequences, as well as the repetitive and the highly similar IS failed to assemble. Otherwise, the SPAdes generated an average 790,468 bp, representing a complete genome with high identity (93%) to other MS sequences available in the Gene Bank [12–16]. Alignment of the draft genomes of MS-H field isolates with that of MS-H exhibited an overall high degree of sequence similarity (99.99%) with no large-scale chromosomal insertions, deletions, duplications or rearrangements except for *vlhA* locus.

The maximum likelihood and NJ analysis performed using platforms REALPHY and MEGA, respectively, on whole genome sequences of 7 MS strains/isolates generated highly comparable results, reflecting a close relationship between MS-H and its field isolates. Notably, MS-H³ and MS-H⁴ were respectively the most closely and distantly related to MS-H (Fig. 1).

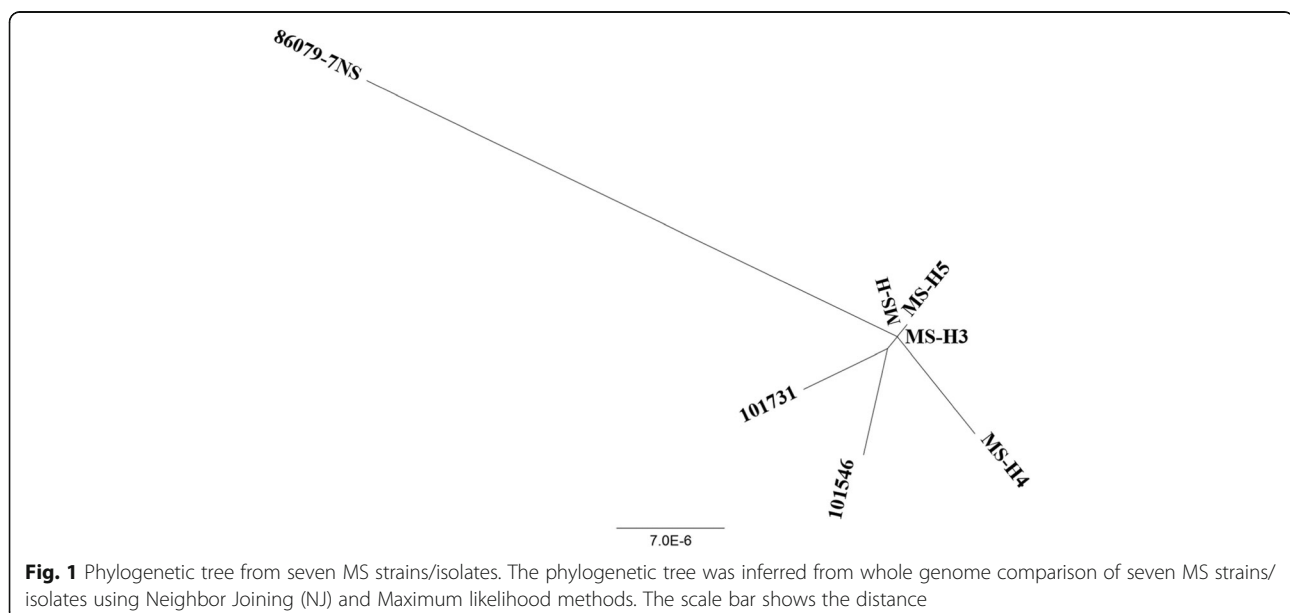


Fig. 1 Phylogenetic tree from seven MS strains/isolates. The phylogenetic tree was inferred from whole genome comparison of seven MS strains/isolates using Neighbor Joining (NJ) and Maximum likelihood methods. The scale bar shows the distance

Table 1 Nucleotide and coding differences identified among the genomes of 86,079/7NS, MS-H and 5 MS-H field isolates

Nucleotide position ^a	86079/7NS	MS-H ^b	MS-H ^{3 b}	MS-H ^{4 b}	MS-H ^{5 b}	101546 ^b	101731 ^b	Protein/region	Functional category	Amino acid change
14181	G	A	A	A	A	A	A	tRNA (Guanine37-N1) methyltransferase	tRNA metabolism	Val→Ile hydrophobic to hydrophobic alkyl to alkyl
36932	A	T	T	T	T	T	T	Non-coding region		
61685	G	A	A	A	A	A	A	DNA topoisomerase IV subunit A	Nucleic acid metabolism	Glu→Lys hydrophilic to hydrophilic acidic to basic
62874	G	A	A	A	A	A	A	Exonuclease ABC subunit UvrB	Nucleic acid metabolism	Gly→Glu hydrophobic to hydrophilic alkyl to acidic
67028	G	A	A	A	A	A	A	tRNA-Trp	tRNA metabolism	
68587	T	T	T	C	T	T	T	Hypothetical protein	Unknown	Synonymous substitution
104704	G	A	A	A	A	A	A	Non-coding region		
107765	G	A	A	A	A	A	A	ABC transporter protein	Transport	Ala→Val hydrophobic to hydrophobic alkyl to alkyl
122053	C	C	C	C	C	T	C	LemA family protein	Unknown	Synonymous substitution
193771	G	A	A	G	G	A	A	GTPase ObgE	Environmental sensing	Gly→Arg hydrophobic to hydrophilic alkyl to basic
194033	C	C	C	C	C	T	T	GTPase ObgE	Environmental sensing	Ala→Val hydrophobic to hydrophobic alkyl to alkyl
200404	T	T	T	A	T	T	T	Hypothetical protein	Unknown	Asp→Val hydrophilic to hydrophobic acidic to alkyl
201094	G	A	A	A	A	A	A	P80-related protein	Unknown	Pro→Ser hydrophobic to hydrophilic alkyl to neutral
203205	C	A	A	A	A	A	A	Non-coding region		
242451	G	A	A	A	A	A	A	NAD-dependent glyceraldehyde -3-phosphate dehydrogenase	Glucose metabolism	Ala→Val hydrophobic to hydrophobic alkyl to alkyl
296526	G	A	A	A	A	G	A	NAD-dependent glyceraldehyde -3-phosphate dehydrogenase	Glucose metabolism	Arg→Lys hydrophilic to hydrophilic basic to basic
316268	T	T	T	T	T	T	—	Hypothetical protein	Unknown	Frame Shift
325032	—	—	—	—	A	—	—	Hypothetical protein	Unknown	Frame Shift
325353	T	T	T	—	T	T	T	Hypothetical protein	Unknown	Frame Shift
352952	G	A	A	A	A	A	A	VACB-like ribonuclease II	Nucleic acid metabolism	Ser→Phe hydrophilic to hydrophobic neutral to aromatic
389629	G	A	A	A	A	A	A	Aspartate-ammonia ligase	Amino acid metabolism	Ala→Thr hydrophobic to hydrophilic alkyl to neutral
397783	T	—	T	T	—	T	T	Peptide ABC transporter ATP-binding protein (OppF)	Transport	Frame Shift
418984	A	A	A	T	A	A	A	TatD family deoxyribonuclease	Nucleic acid metabolism	Asp→Val hydrophilic to hydrophobic acidic to alkyl
433343	G	A	A	A	A	A	A	Alanine tRNA ligase	tRNA metabolism	Asp→Asn hydrophilic to hydrophilic acidic to neutral
438657	G	A	A	A	A	A	A	Triacylglycerol lipase	Lipid metabolism	Synonymous substitution

Table 1 Nucleotide and coding differences identified among the genomes of 86,079/7NS, MS-H and 5 MS-H field isolates (Continued)

Nucleotide position ^a	86079/7NS	MS-H ^b	MS-H ^{3 b}	MS-H ^{4 b}	MS-H ^{5 b}	101546 ^b	101731 ^b	Protein/region	Functional category	Amino acid change
449402	G	G	G	A	G	G	G	Cardiolipin synthetase	membrane lipid	Ala→Thr hydrophobic to hydrophilic alkyl to neutral
449694	G	G	G	G	G	G	A	Cardiolipin synthetase	membrane lipid	Ser→Asn hydrophilic to hydrophilic neutral to neutral
457951	G	G	G	G	G	G	A	Hypothetical protein	Unknown	Synonymous substitution
481287	G	A	A	A	A	A	A	Haemolysin C or DUF21 domain- containing protein	Structural Protein	Ala→Val hydrophobic to hydrophobic alkyl to alkyl
485166	C	C	C	C	T	C	C	DHH subfamily	Phosphoesterase function	Synonymous substitution
498421	T	C	C	C	C	C	C	Histidyl-tRNA synthetase	tRNA metabolism	Thr→Ala hydrophilic to hydrophobic neutral to alkyl
502825	AT	AT	AT	AT	—	AT	AT	Non-coding region		
502827	AT	—	—	AT	—	—	AT	Non-coding region		
502829	—	—	—	AT	—	—	—	Non-coding region		
510721	G	G	G	A	G	G	G	Thymidine phosphorylase	Pyrimidine metabolism	Synonymous substitution
522899	G	A	A	A	A	A	A	Hypothetical protein	Unknown	Gly→Glu hydrophobic to hydrophilic alkyl to acidic
553886	C	C	C	C	C	T	C	Hypothetical protein	Unknown	Ala→Thr hydrophobic to hydrophilic alkyl to neutral
563391	G	A	A	A	A	A	A	Hexosephosphate transport protein	Transport	Leu→Phe hydrophobic to hydrophobic alkyl to aromatic
567729	C	A	A	A	A	A	A	DNA-directed RNA polymerase beta' subunit	Nucleic acid metabolism	Arg→Ile hydrophilic hydrophobic basic to alkyl
572029	T	T	T	T	T	T	C	DNA-directed RNA polymerase subunit beta	Nucleic acid metabolism	Glu→Gly hydrophilic to hydrophobic acidic to alkyl
584838	G	A	A	A	A	A	A	Hypothetical protein	Unknown	Synonymous substitution
604569	C	C	C	C	C	A	C	Hypothetical protein	Unknown	Asp→Glu hydrophilic to hydrophilic acidic acidic
615741	G	A	A	A	A	A	A	Potassium uptake protein KtrB	Transport	His→Tyr hydrophilic to hydrophilic basic to neutral
628272	G	A	A	A	A	A	A	DNA polymerase III alpha subunit	Nucleic acid metabolism	Ser→Phe hydrophilic to hydrophobic neutral to aromatic
637130	G	G	G	G	G	A	G	YbhB/YbcL family Raf kinase inhibitor-like protein	Protease inhibitor	Val→Ile hydrophobic to hydrophobic alkyl alkyl
651973	C	C	C	A	C	C	C	S1 RNA-binding domain-containing protein	RNA metabolism	Ser→Ile hydrophilic to hydrophobic neutral to alkyl
679814	G	A	A	A	A	A	A	Cation-transporting P- type ATPase	Transport	Synonymous substitution
686265	G	A	A	A	A	A	A	Non-coding region		
716623	G	A	A	A	A	A	A	Hypothetical protein	Unknown	Ser→Leu hydrophilic to hydrophobic neutral to alkyl

Table 1 Nucleotide and coding differences identified among the genomes of 86,079/7NS, MS-H and 5 MS-H field isolates (Continued)

Nucleotide position ^a	86079/7NS	MS-H ^b	MS-H ³ ^b	MS-H ⁴ ^b	MS-H ⁵ ^b	101546 ^b	101731 ^b	Protein/region	Functional category	Amino acid change
737180	G	A	A	A	A	A	A	Hypothetical protein	Unknown	Synonymous substitution
780235	AT	AT	AT	—	AT	AT	AT	Non-coding region		
780237	AT	—	—	—	—	—	—	Non-coding region		
794057	G	A	A	A	A	A	A	Uridine monophosphate kinase	Central metabolism	His→Tyr hydrophilic to hydrophilic basic to neutral

* *vihA* locus was excluded from SNP analysis

^a Nucleotide position corresponding to the MS-H genomic sequence (Genbank accession no. CP021129)

^b “—” indicates absence of nucleotide(s)

Of the 32 mutations previously found between 86,079/7NS and MS-H, only four were observed to have reversed Comparative genomic analysis found a total of 25 SNP and indel variants between MS-H and its field isolates (Table 1). MS-H⁴ and MS-H³ had the highest (12) and the lowest (1) number of genomic differences with MS-H, respectively, while MS-H⁵, 101,546 and 101,731 had 4, 7 and 7 differences, respectively. Four out of these 25 SNPs had been detected in a previous study that compared the genomes of MS-H and its parent strain 86,079/7NS [12], however the other 21 were found only in the 5 reisolates.

The MS-H³ had an identical sequence to MS-H except for the coding DNA sequence (CDS) of *oppF* in which insertion of ‘T’ at position 468 resulted in the restoration of the full-length *oppF* sequence identical to that of 86,079/7NS.

Three non-synonymous differences were found between genomes of MS-H and MS-H⁵. These included deletion of two nucleotides ‘AT’ in a tandem repeat in a non-coding region (positions 502,825) upstream of the cytosine-5-methyltransferase CDS, insertion of nucleotide ‘A’ (causing frame-shift mutation) in a gene (CDS 164) encoding a protein of unknown function, and nucleotide substitution ‘A’ to ‘G’ in *obg* gene resulting in restoration of the wild-type Obg (Arg123Gly). Also, a synonymous substitution (‘C’ to ‘T’) in Glu322 was found in the CDS 966 which codes for Desert Hedgehog Signalling Molecule.

Twelve genomic differences were found between MS-H⁴ and MS-H, three of which had been described to exist between MS-H and 86,079/7NS and were reverted to wild-type sequence. These comprised of insertion of ‘AT’ at position 502,827 in a tandem repeat within a non-coding region, a SNP in *obg* gene (similar to that found in MS-H³) and a frameshift mutation in the *oppF* gene (identical to that found in MS-H³). The other 9 mutations comprised of 6 in genes coding for Cardiolipin, two hypothetical protein, TatD deoxyribonuclease, S1 RNA-binding domain, and Thymidine phosphorylase, 1 in a gene with unknown function, 2 in non-coding regions.

In the isolate 101,546, two genomic differences were found to cause reversion to wild-type sequence. These included ‘A’ to ‘G’ in *gap* gene (at CDS 554) which resulted in a conservative change (Ala185Val), and a frameshift mutation in *oppF* identical to that from MS-H³ and MS-H⁴. Moreover, four non-synonymous substitutions were found in CDSs corresponding to Obg, YbhB/YbcL Raf kinase inhibitor, and two hypothetical proteins. These substitutions were due to ‘C’ to ‘T’ at CDS 629 in *obg* gene resulting in a conservative change (Ala210Val); ‘C’ to ‘A’ at CDS 909 causing a conservative change (Asp303Glu) in a gene encoding a hypothetical protein; ‘G’ to ‘A’ at CDS 220 resulting a conservative change (Val74Ile) in gene encoding YbhB/YbcL Raf kinase inhibitor, and ‘C’ to ‘T’ at CDS 3979 resulting in a non-conservative substitution (Ala1327Thr). Moreover, a synonymous substitution in Thr197 was found in CDS corresponding to LemA (‘C’ to ‘T’ at CDS 591).

Comparison of MS-H and 101,731 were found changes in *obg* and *oppF* genes consistent with those of 1,015,465. Moreover, similar to MS-H⁴, ‘AT’ insertions at positions 502,827 was found resulting in reversion to wild-type sequence. In addition, a ‘T’ deletion at CDS 387 in a gene encoding a hypothetical protein, substituted Tryr135 to a premature stop-codon. Moreover, genes encode Cls and DNA-directed RNA polymerase subunit beta were found to have a ‘G’ to ‘A’ substitution which resulted in a conservative amino acid change (Ser263-Asn), and a ‘T’ to ‘C’ substitution which resulted in a non-conservative substitution (Glu1037Gly), respectively. Additionally, a synonymous substitution in Asx362 was found in CDS corresponding to a hypothetical protein (‘G’ to ‘A’ at CDS 1086).

Mutations found in genes coding for Obg, OppF, Cardiolipin, and YbhB/YbcL Raf kinase-inhibitor were computationally predicted to affect the proteins structure The final alignment between targeted proteins and templates using Phyre2 for eight proteins (OppF, Obg, Cls, TatD, S1 RNA-binding, NAD-dependent glyceraldehyde-3-phosphate dehydrogenase, YbhB/YbcL Raf kinase

Table 2 Homology modelling results of proteins vary between MS-H and its field isolates

Gene locus-tag	Percentage of residues modelled at > 90% confidence	Protein product in MS-H	Protein effect	Model template library ID	MS-H vs. isolates	Secondary structure prediction ^a			Protein length (amino acid)	Mutational sensitivity ^b (potential functional/phenotypic effect)
						α helix %	β strand %	Different structure		
MSH_RS00965	99	GTP-binding protein Obg	Non-conservative substitution	c1udxA	MS-H	26	26	Yes	424	Low
					MS-H4, MS-H5	29	26			
MSH_RS00965	99	GTP-binding protein Obg	Conservative substitution	c1udxA	MS-H	26	26	No	424	Medium
MSH_RS01740	91	Peptide ABC transporter ATP-binding protein	Frameshift	c5ws4A	MS-H	31	24	Yes	156	High
					MS-H3, MS-H4-101546-101731	68	7		796	
MSH_RS01990	75	Cardiolipin synthetase	Non-conservative Substitution	c3hsiC	MS-H	50	17	Yes	504	High
					MS-H4	51	17			
MSH_RS00995	0	Hypothetical protein	Non-conservative substitution	c2yu6A	MS-H	65	8	No	398	NA
					MS-H4	65	8			
MSH_RS01480	0	Hypothetical protein	Frameshift	d1r5qa	MS-H	–	–	–	166	NA
				d1r8ja1	MS-H4				161	
MSH_RS01480	0	Hypothetical protein	Frameshift	d1r5qa	MS-H	–	–	–	166	NA
				c3kbIA	MS-H5				56	
MSH_RS01835	100	TatD family deoxyribonuclease	Non-conservative substitution	c3ipwA	MS-H	47	16	No	268	Low
					MS-H4	47	16			
MSH_RS02805	100	S1 RNA-binding domain-containing protein	Non-conservative substitution	c2oceA	MS-H	55	10	Yes	705	Low
					MS-H4	56	10			
MSH_RS01365	100	NAD-dependent glyceraldehyde -3-phosphate dehydrogenase	Conservative substitution	c3hq4R	MS-H	27	31	Yes	334	Low
					101546	27	32			
MSH_RS02615	37	Hypothetical protein	Conservative substitution	c6dgvA	MS-H	55	7	No	651	Medium
					101546	55	7			
MSH_RS02750	91	YbhB/YbcL family Raf kinase inhibitor-like protein	Conservative substitution	c2evdD	MS-H	6	23	No	221	High
					101546	6	23			
MSH_RS02415	0	Hypothetical protein	Non-conservative substitution	c5il9A	MS-H	22	38	–	1575	NA
					101546	–	–			
MSH_RS01430	16	Hypothetical protein	Frameshift	c4aq4A	MS-H	36	12	Yes	797	Low
				d1tdpa	101731	44	17		405	
MSH_RS01990	75	Cardiolipin synthetase	Conservative substitution	c3hsiC	MS-H	50	17	No	504	Low
					101731	50	17			
MSH_RS02470	92	DNA-directed RNA polymerase subunit beta	Non-conservative substitution	c3lu0C	MS-H	33	25	No	1202	Low
					101731	33	25			

^a "Yes" indicates different secondary structure of respective protein between MS-H and its reisolates; "No" shows that MS-H and its reisolates have the same secondary structure of the respective protein; "–" indicates that only a domain of respective protein was modelled and as the result the percentage of α helix and β strand were not reliable

^b "High" indicates that respective mutation highly likely has functional/phenotypic effect; "Medium" shows that respective mutation moderately likely has functional/phenotypic effect; "Low" shows that respective mutation has low potential functional/phenotypic effect; "NA" indicates that position corresponding to respective mutation was not modelled

inhibitor and DNA-directed RNA polymerase subunit beta) exhibited an average 76% of residues modelled at 100% confidence. For the other five proteins (hypothetical proteins) only an average 40% of residues modelled at > 50% confidence and none of residues modelled at > 90% confidence (Table 2). The model template IDs, protein lengths, predicted secondary structures, and the degree (%) of mutation sensitivity at a given position in the respective proteins are detailed in Table 2.

Consistent with findings from a previous study [8], homology modelling of Obg in MS-H showed that Arg123 is located in large pocket region, which are frequently the active sites [17], however the probability that a missense mutation at this position effecting function of the corresponding protein was predicted low. The percentages of predicted alpha helices in the Obg protein sequences of MS-H⁴ or MS-H⁵ (29%), was different from that of MS-H (26%), due to the Arg123Gly difference between these strains. By contrast, the Ala210Val difference in the Obg protein sequence of strains 101,546 and 101,731 did not change the secondary structure of Obg compared to that of MS-H.

The frameshift mutation corresponding to *oppF* gene in MS-H³, MS-H⁴, 101,546 and 101,731 restored the full-length OppF (reversion to wild-type). Based on the protein homology analysis conducted as part of this study, the functional domain of OppF is identified at the

C terminus. As a result, the secondary structure of OppF in above-mentioned isolates (which possessed 68% alpha helices and 7% beta strands) was significantly different to that of MS-H (31% alpha helices and 24% beta strands).

Residue 166 in Cls of MS-H is in a highly sensitive mutation region and therefore Ala166Thr in MS-H⁴ was predicted to affect its function. Also, due to this amino acid change, the secondary structure of Cls in MS-H⁴ (containing 51% alpha helices) was different to that of MS-H (containing 50% alpha helices). By contrast, amino acid at position 263 was in a low mutation sensitive region. Therefore, Ser263Asn was unlikely to affect the protein Cls function in isolate 101,731. Also, the secondary structure of Cls in 101,731 was modelled identical to that from MS-H.

The TatD deoxyribonuclease and S1 RNA-binding proteins were also modelled and compared between MS-H and MS-H⁴ for their mutations at positions 143 and 57, respectively. In MS-H both these mutations were in low sensitive mutation regions and therefore were unlikely to affect the function of the respective proteins in MS-H⁴. However, the latter substitution resulted in a slight change in the percentage of alpha helices from 55% in MS-H to 56% in MS-H⁴, and this could potentially alter the secondary structure of the protein.

The Arg185 in NAD-dependent glyceraldehyde-3-phosphate dehydrogenase in MS-H was in a low mutation sensitive region. The Arg185lys could potentially

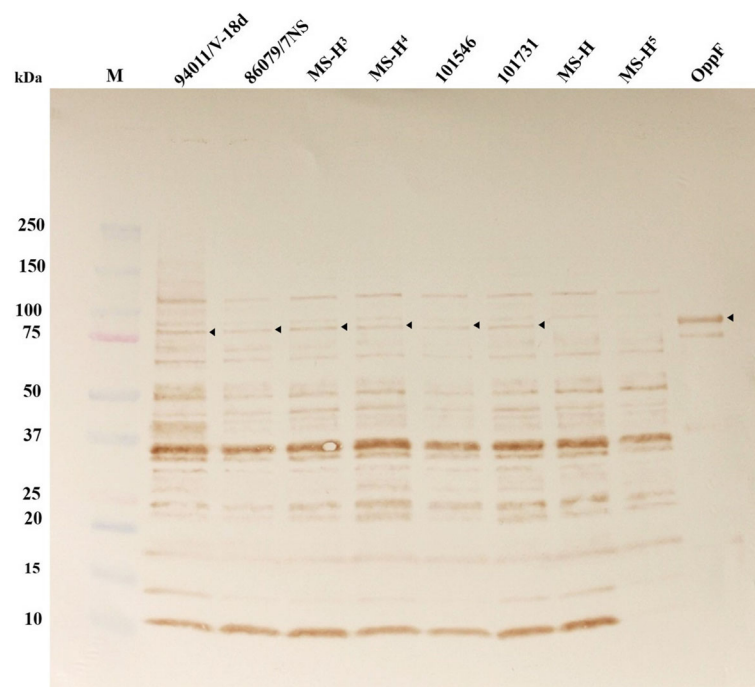


Fig. 2 Analysis of OppF expression in MS strains/isolates. Western Immunoblots of recombinant purified OppF and whole-cell lysate from MS strains/isolates probed with rabbit-anti-OppF-N. The arrow heads show the location of full-length OppF. M is Precision Plus protein TM, Dual Color marker (Bio-Rad)

change the secondary structure of the protein in 101,546 compared to that of MS-H as the percentage of beta strands changed from 31% in MSH to 32% in 101,546.

The protein YbhB/YbcL Raf kinase inhibitor was also modelled in MS-H and 101,546. Residue Val74 was found in a highly sensitive mutation region and therefore Val74Ile could potentially affect the function of the respective protein in 101,546. The secondary structure of this protein was identical in MS-H and 101,546.

The effect of Glu1037Gly in DNA-directed RNA polymerase subunit beta in 101,731 was found neutral as Glu1037 was located in a low sensitive mutation site and the secondary structure of respective protein was identical in MS-H and 101,731.

Full-length OppF was detected in all MS-H reisolates

Amongst all mutations detected in MS-H reisolates, the frameshift mutation in the *oppF* gene appeared to have the most significant impact on the structure of its encoded protein and therefore was further investigated. The wild-type *oppF* was predicted to encode a polypeptide of 797 amino acids (approximately 94 kDa). Immunoblotting experiments with rabbit-anti-OppF-N antibodies detected the OppF protein of expected size (~ 94 kDa) in 86,079/7NS, MS-H³, MS-H⁴, 101,546 and 10,173,118, while did not detect any protein of similar size in MS-H and MS-H⁵ cells (Fig. 2). The rabbit-anti-OppF-N antibodies also detected several presumably nonspecific bands of similar sizes in all MS strains/isolates lysates tested.

Discussion

This is the first study that investigates the stability of all mutations in a live attenuated mycoplasma vaccine after in vivo passage under field conditions. The initial swab cultures collected from MS-H vaccinated birds were passaged three times in vitro by selection of an individual colony from each step. It may be possible that in vitro passage of the clones may have incorporated selection pressure and bias into the expansion of a clonal population, however it is notable that the clones were compared against an in vitro propagated MS-H vaccine strain. Whole genome sequencing directly from clinical materials collected from vaccinated birds would be ideal to circumvent the potential of in vitro selection pressure, but currently available does not allow compilation of complete genome sequence reliable at a base pair level. Also, current techniques may run the risk of generating a chimeric genome generated from multiple clonal populations that may cohabit the bird's respiratory system.

A recent study [12] described 32 mutations within the MS-H genome as compared to its parent strain 86,079/7NS. However, the stability of these mutations after

passage in vivo had only been tested for those found in *obg* [8] and *oppF* [9].

Protein homology modelling found that four sequence variations between MS-H and reisolates from vaccinated flocks, located in genes coding for Obg, OppF, Cardiolipin, and YbhB/YbcL Raf kinase-inhibitor, were likely to affect the in vitro and/or in vivo characteristics of MS.

Given that *oppF* is involved in pathogenesis of *M. bovis* [10], and the wild-type OppF from MS shares 43% amino acid similarity with that of *M. bovis*, the genomes of five MS-H field isolates differing in the *oppF* gene with that from MS-H and 86,079/7NS was analysed in this study to reflect the possible role of *oppF* in temperature sensitivity/attenuation phenotype of MS-H. Mycoplasmas can survive in vivo due to complex interaction between the microorganism and the host environment [18]. A continuous source of a nutrient used by a gene that is essential for in vivo survival may be a vital factor in the capability of a pathogen to cause disease [10]. Several nutrients are gained from exogenous sources by mycoplasmas as a result of their limited synthesis pathways. Hence, the ability to integrate molecules over membrane-associated transport systems appears to be a substantial factor for in vivo survival of mycoplasmas. In *M. bovis*, two transporters (oligopeptide transporter *oppABCDF* and an uncharacterized transporter) were essential for colonization on the tracheal mucosa [10]. In *M. mycoides* subsp. *mycoides*, a glycerol transporter (*gtsABC*) has been specified as a virulence factor related with hydrogen peroxide production and induction of cytotoxicity [19–21]. The level of mRNA expression of *oppD* of *M. hyopneumoniae* was moderately up-regulated throughout in vivo infection [22] and under iron-depletion conditions [23]. Therefore, all available studies on the role of OppF in several *Mycoplasma species* are highly suggestive that OppF has a major contribution to the attenuation of MS-H. It is notable that in Western Immunoblot analysis conducted as part of this study, the truncated OppF was not detectable in MS-H and MS-H⁵ (Fig. 2). It is speculated that the truncated version of OppF does not react well with polyclonal antibody against N terminus of OppF. The repeat of this Western Immunoblot in this and our previous publication [24] has shown that truncated version of OppF has only minimal reaction against anti-OppF-N polyclonal antibody. It is postulated that most of epitopes of this antibody are probably conformational (as opposed to linear) and may require of the remaining OppF protein to fully react and provide a readily detectable band on Western Immunoblot.

In bacteria, the Cardiolipin levels have been found to elevate in the stationary growth phase due to up-regulation of Cls activity in response to osmotic stress [25]. The importance of anionic phospholipids cl in the

osmotic adaptation and in the membrane structure of *Bacillus subtilis* cultures was demonstrated by impairment of osmotolerance in a Cls mutant (*clsA*) of this organism. As well as the lack in *cl* synthesis, this mutant indicated other deficiencies in lipid and fatty acid content compared to the wild-type, signifying a cross-regulation in membrane lipid pathways, critical for the conservation of membrane functionality and integrity [25]. Therefore, it appears that elucidation of the role of Cardiolipin in attenuation of MS-H needs further investigation.

Given that the amino acid substitution in Cls of MS-H⁴ was predicted to change secondary structure of the respective protein compared to that of MS-H and mutation resides in a highly sensitive mutation region, it is likely that this mutation affects the function of the respective protein in MS-H⁴.

The two proteins YbhB and YbcL belong to Raf kinase family and play role in the regulation of protein phosphorylation by kinases in *E. coli* [26]. Phosphorylation and dephosphorylation of proteins play a fundamental role in signalling in bacteria [27, 28]. Previous studies have confirmed the significance of the phosphorylation of threonine and histidine residues and serine/threonine kinases which were involved in pathogenicity and stress responses in several prokaryotes [29]. Although the Val74Ile substitution in YbhB/YbcL of isolate 101,546 was unlikely to influence the secondary structure of the respective protein, it was found in a highly sensitive mutation region and therefore could affect the function of this protein.

Earlier studies in our laboratory have revealed that GapA⁺ *M. gallisepticum* (MG) ts-11 vaccine was more immunogenic and induced higher antibody response than the GapA⁻ ts-11 population [30]. In MG, the GapA is determined as the primary cytoadhesin molecule and is known to play role in prolonged colonization and survival of MG [31, 32]. Interestingly, isolate 101,546 was recovered from a MS-H vaccinated flock with unusually high systemic antibody response to MS. This isolate had a mutation in NAD-dependent glyceraldehyde-3-phosphate dehydrogenase, located in large pocket regions and found likely to change the secondary structure of the respective protein compared to that of MS-H.

Comparative analysis of the genomes of selected MS isolates from MS-H vaccinated flocks revealed that they were true reisolates of the MS-H vaccine as they had highly similar genome to that of MS-H as opposed to 86,079/7NS. Results of this study also demonstrated that out of 32 mutations found in MS-H genome [12], only four to be reversible (Table 1) after passage in field birds. Thus, the 28 other mutations appear to be stable in MS-H. Of the four unstable mutations, two (found in the *Obg* and *OppF*), were predicted to have some effects on MS virulence.

The mutations which are prone to revert are those that provide advantages to the organism to grow faster or grow in different parts of the respiratory system. For example, reversion mutations in *obg* provide organism higher capacity to live in lower respiratory system or mutation in *oppF* provides organism utilising amino acids more efficiently. These are important to drive reversion to wild-type organism. The mutations that were not found to revert organism to wild-type state probably do not provide the vaccine a significant advantage in vivo.

Given that obtaining pure cultures of the MS-H reisolates characterised here had to undergo multiple steps of growing in liquid and solid media, it may be possible that some of the mutations detected were as a result of in vitro passage. Future studies should therefore target these mutations directly in clinical specimens collected from vaccination chickens.

The data generated in this study also set the foundation for future research aiming to develop strain identification tests that reliably distinguish MS-H from other MS strains that possess identical *vlhA* gene sequence. Furthermore, using a set of mutations found here, it may be possible to correlate results emerging from genotyping techniques to variations in characteristics of MS isolates.

Conclusion

Results of this study reveal that most of the MS-H mutations are stable after passage in vaccinated chickens. Characterisation of stable mutations observed in MS-H could be applied to develop rapid diagnostic techniques for differentiation of vaccine from field strains or *ts*-MS-H reisolates.

Methods

MS strains, growth conditions, and DNA extraction

All MS-H isolates used in this study (Table 3) were made from flocks vaccinated with MS-H at various times after vaccination. All initial swab cultures were cloned by selection of individual colonies three times. The MS-H isolates were grown in mycoplasma broth supplemented with 10% swine serum (Sigma-Australia) and 0.01% (w/v) of nicotinamide adenine dinucleotide (NAD) (Sigma-Australia) [33] at 37 °C in a 50 mL final volume until late logarithmic phase (approximately pH 6.8). Cells were collected followed by extraction of genomic DNA as described previously [12]. The DNA concentration was measured using the optical density at 260 nm (OD₂₆₀) using a NanoDrop™ 2000c spectrophotometer (Thermo Fisher Scientific, Waltham, MA, USA) and purity was evaluated by calculating the OD_{260/280} ratio. The integrity of DNA was assessed using chromatography through 0.8% agarose gel and DNA products were stored at - 80 °C until use.

Table 3 Summary of the isolates examined in this study

Strain/isolate	Source	Date collected	Origin	Reference
94011/V-18d	Broiler breeder	1998	MS field strain, poultry farm, Victoria, Australia	[7]
86079-7NS	Layer breeder	1998	Parent strain of MS-H vaccine, palatine cleft, poultry farm, Victoria, Australia	[6]
MS-H	Vaxsafe MS*	2005	Vaccine strain derived from 86079/7NS, Bioproperties Pty. Ltd., Ringwood, Victoria, Australia	[6]
MS-H ³	Broiler breeder	1998	MS-H-vaccinated flock, poultry farm, Victoria, Australia	[6]
MS-H ⁴	Broiler breeder	1998	MS-H-vaccinated flock, poultry farm, Victoria, Australia	[6]
MS-H ⁵	Broiler breeder	1998	MS-H-vaccinated flock, poultry farm, Victoria, Australia	[6]
101546	Broiler breeder	2016	MS-H-vaccinated flock, poultry farm, New South Wales, Australia	This study
101731	Broiler breeder	2016	MS-H-vaccinated flock, poultry farm, Victoria, Australia	This study

Next-generation sequencing (NGS)

NGS of all MS-H field isolates was performed using Paired-end 125-bp reads by the Illumina MiSeq platform at the Australian Genome Research Facility Ltd. (AGRF, Melbourne, VIC, Australia).

De novo assembly and sequence analysis

SPAdes assembler version 3.10.0 (Geneious® version 11.1.3) was used to perform De Novo assembly of contiguous sequences. To visualize overall sequence similarity and identify genomic organisation between the MS-H and its field isolates, the contigs were aligned to MS-H genome (GenBank accession number CP021129) as reference using Mauve (Mauve Contig Mover (MCM)), Geneious®. The MCM aligns a draft genome to a reference sequence and orders the contigs in the draft genome according to their position along the reference genome [34, 35].

The resulting contigs and Illumina short reads were mapped to the MS-H genome using Geneious as mapper in Geneious®. Subsequently the alignments were subjected to single nucleotide polymorphism (SNP) and insertion/deletion (indel) analysis. To detect SNPs and indels, 'Find Variations/SNPs' in Geneious® was used.

The genome sequence of strain 86,079/7NS (GenBank accession numbers NZ_CP012624) was also included as reference for analysis of SNPs.

Phylogenetic analysis

To establish the relationship of MS-H isolates (GenBank accession number PRJNA649354), MS-H (GenBank accession number CP021129.1) and 86,079/7NS (GenBank accession number CP012624.1), their whole genome sequence were analysed using maximum likelihood and Neighbor Joining (NJ) methods and the DNA evolutionary models including GTR+ G+ I (GTR: General Time Reversible; G: Gamma distribution; I: evolutionary invariable) and HKY85 (Hasegawa-Kishino-Yano) employing two programs REALPHY (version 1.12) [36] and MEGA (version 10) [37].

Homology modelling of proteins vary between isolates

The Phyre2 (protein homology/analogy recognition engine V 2.0) web portal for protein modelling, prediction and analysis (<http://www.sbg.bio.ic.ac.uk/~phyre2/html/page.cgi?id=index>) [38] was used for homology modelling of proteins deduced from genes harboured SNP and indel variants in MS-H field isolates. Intensive mode of modelling was selected which performs complete modelling of the entire protein using multiple templates and ab initio techniques. Furthermore, the resultant modelled protein was subjected to Phyre investigator for more in-depth analysis [39].

The crystal structure of the GTP-binding protein Obg from *Thermus thermophilus* (protein data bank (PDB) ID: c1udxA), ATP-binding/permease from *Acinetobacter baumannii* (PDB ID: c5ws4A), Cardiolipin synthetase (Cls) from (PDB ID: c3hsiC), hydrolase TatD family protein from *Entamoeba histolytica* (PDB ID: c3ipwA), Tex family protein pa5201 from *Pseudomonas aeruginosa* (PDB ID: c2oceA), Glyceraldehyde-3-phosphate dehydrogenase from *Staphylococcus aureus* (PDB ID: c3hq4R), Pebp-like protein hp02182 from *Helicobacter pylori* (PDB ID: c2evvD), and DNA-directed RNA polymerase subunit beta from *Escherichia coli* (PDB ID: c3lu0C) were determined and used as homology models for Obg, OppF, Cls, TatD deoxyribonuclease, S1 RNA-binding domain, NAD-dependent glyceraldehyde-3-phosphate dehydrogenase, YbhB/YbcL Raf kinase inhibitor and DNA-directed RNA polymerase subunit beta, respectively.

Detection of OppF expression in MS strains/isolates

One ml volumes of mycoplasma broth were inoculated with 1/10 dilution of MS strains/isolates (Table 3) and grown to late exponential phase (~ pH 6.8). The cells were treated as described previously [24] and subjected to sodium dodecyl sulfate–polyacrylamide gel electrophoresis (SDS-PAGE) followed by Immunoblotting with mono-specific rabbit sera raised against N terminus of OppF [24].

The MS 94011/V-18d and 86,079/7NS possessing full-length *oppF*, MS-H possessing truncated *oppF*, and recombinant purified OppF [24] were used as controls.

Abbreviations

MS: *Mycoplasma synoviae*; ts +: Temperature sensitive; ts -: Non- temperature sensitive; *opp*: Oligopeptide permease; CDS: Coding DNA sequence; w: Wild-type; v: Vaccine-type; MG: *M. gallisepticum*; NGS: Next-generation sequencing; MCM: Mauve Contig Mover; NJ: Neighbor Joining; GTR+ G+ I: General Time Reversible+ Gamma distribution+ evolutionary invariable; HKY85: Hasegawa-Kishino-Yano; Phyre2: Protein homology/analogy recognition engine V 2.0; PDB: Protein data bank; PBS: Phosphate buffered saline; SDS: Sodium dodecyl sulfate; SDS-PAGE: Sodium dodecyl sulfate–polyacrylamide gel electrophoresis

Acknowledgments

Authors acknowledge the assistance of the staff from Asia-Pacific Centre for Animal Health (APCAH), Veterinary School, Faculty of Veterinary & Agricultural Sciences, The University of Melbourne, Australia. Authors also thank Dr. Chris Morrow, Bioproperties Pty. Ltd. for proofreading of the manuscript.

Authors' contributions

All authors have read and approved the final manuscript. AN and SK conceived the idea, designed the study and interpreted the results. SK conducted the laboratory work and analysed the data and drafted the manuscript. Bioinformatics analysis: SK, AN and MM. Acquisition, analysis, technical assistance and advice on the structure of the manuscript: PS, OO, BK and JD.

Funding

Financial support to conduct this study was provided by the Asia-Pacific Centre for Animal Health (APCAH). The funder had no role in study design, data collection and analysis, decision to publish, or preparation of the manuscript.

Availability of data and materials

The datasets generated and/or analysed during the current study are available in the GenBank repository. The Sequence Read Archive (SRA) of the five selected field reisolates of vaccine strain MS-H has been deposited in GenBank under accession number PRJNA649354 [MS-H³: SRX8841481; MS-H⁴: SRX8841482; MS-H⁵: SRX8841483; 101564: SRX8841484 and 101731: SRX8841485]. The genome sequences of MS-H and 86079/7NS were retrieved from GenBank (accession numbers CP021129.1 and CP012624.1).

Ethics approval and consent to participate

There was no ethics approval required for this study. All samples were submitted to APCA by the poultry companies/farms as part of their diagnostic and monitoring activities.

Consent for publication

Not applicable.

Competing interests

The authors have declared no conflict of interest.

Received: 3 June 2020 Accepted: 17 August 2020

Published online: 28 August 2020

References

- Catania S, Bilato D, Gobbo F, Granato A, Terregino C, Iob L, et al. Treatment of eggshell abnormalities and reduced egg production caused by *Mycoplasma synoviae* infection. Avian Dis. 2010;54(2):961–4.
- Ferguson-Noel N, Noormohammadi AH. *Mycoplasma synoviae* infection. In: Swayne DE, Glisson JR, McDougald LR, Nolan LK, Suarez DL, Nair VL, editors. Diseases of Poultry. 13th ed. Hoboken: Wiley-Blackwell; 2013. p. 875.
- Morrow CJ, Markham JF, Whithear KG. Production of temperature-sensitive clones of *Mycoplasma synoviae* for evaluation as live vaccines. Avian Dis. 1998;42(4):667–70.
- Cruz-Vera LR, Toledo I, Hernandez-Sanchez J, Guarneros G. Molecular basis for the temperature sensitivity of *Escherichia coli* pth (Ts). J Bacteriol. 2000; 182(6):1523–8.
- Haga T, Murayama N, Shimizu Y, Saito A, Sakamoto T, Morita T, et al. Analysis of antibody response by temperature-sensitive measles vaccine strain in the cotton rat model. Comp Immunol Microb. 2009;32(5):395–406.
- Markham JF, Scott PC, Whithear KG. Field evaluation of the safety and efficacy of a temperature-sensitive *Mycoplasma synoviae* live vaccine. Avian Dis. 1998;42(4):682–9.
- Noormohammadi AH, Jones JF, Harrigan KE, Whithear KG. Evaluation of the non-temperature-sensitive field clonal isolates of the *Mycoplasma synoviae* vaccine strain MS-H. Avian Dis. 2003;47(2):355–60.
- Shahid MA, Markham PF, Markham JF, Marenda MS, Noormohammadi AH. Mutations in GTP binding protein Obg of mycoplasma synoviae vaccine strain MS-H: implications in temperature-sensitivity phenotype. PLoS One. 2013;8(9):e73954.
- Zhu L, Kongsak BM, Olaogun OM, Agnew-Crumpton R, Kanci A, Marenda MS, et al. Identification of a new genetic marker in *Mycoplasma synoviae* vaccine strain MS-H and development of a strategy using polymerase chain reaction and high-resolution melting curve analysis for differentiating MS-H from field strains. Vet Microbiol. 2017;210:49–55.
- Lee N. Characterization of an ATP-binding cassette (ABC) transport system involved in nucleoside uptake in *Mycoplasma bovis* strain M23, and discovery of its pathogenicity genes, in Iowa State University, Ames, Iowa; 2009.
- Tseng CW, Chiu CJ, Kanci A, Citti C, Rosengarten R, Browning GF, et al. The *oppD* gene and putative peptidase genes may be required for virulence in *Mycoplasma gallisepticum*. Infect Immun. 2017;85(6):e00023–17.
- Zhu L, Shahid MA, Markham J, Browning GF, Noormohammadi AH, Marenda MS. Comparative genomic analyses of *Mycoplasma synoviae* vaccine strain MS-H and its wild-type parent strain 86079/7NS: Implications for the identification of virulence factors and applications in diagnosis of *M. synoviae*. Avian Pathol. 2019;48(6):537–48.
- Bumgardner EA, Kittichotirat W, Bumgarner RE, Lawrence PK. Comparative genomic analysis of seven *Mycoplasma hyosynoviae* strains. Microbiologyopen. 2015;4(2):343–59.
- Himmelreich R, Hilbert H, Plagens H, Pirkl E, Li BC, Herrmann R. Complete sequence analysis of the genome of the bacterium *Mycoplasma pneumoniae*. Nucleic Acids Res. 1996;24(22):4420–49.
- Sasaki Y, Ishikawa J, Yamashita A, Oshima K, Kenri T, Furuya K, et al. The complete genomic sequence of *Mycoplasma penetrans*, an intracellular bacterial pathogen in humans. Nucleic Acids Res. 2002;30(23):5293–300.
- Zhu L, Shahid MA, Markham J, Browning G, Noormohammadi AH, Marenda M. Genome analysis of *Mycoplasma synoviae* strain MS-H, the most common *M. synoviae* strain with a worldwide distribution. BMC Genomics. 2018;19:117.
- Le Guilloux V, Schmidtke P, Tuffery P. Fpocket: an open source platform for ligand pocket detection. Bmc Bioinformatics. 2009;10:168.
- Lipsitch M, Moxon ER. Virulence and transmissibility of pathogens: what is the relationship? Trends in Microbiol. 1997;5(1):31–7.
- Hames C, Halbedel S, Hoppert M, Frey J, Stulke J. Glycerol metabolism is important for cytotoxicity of *Mycoplasma pneumoniae*. J Bacteriol. 2009; 191(3):747–53.
- Pilo P, Vilei EM, Peterhans E, Bonvin-Klotz L, Stoffel MH, Dobbelaere D, et al. A metabolic enzyme as a primary virulence factor of *Mycoplasma mycoides* subsp mycoides small colony. J Bacteriol. 2005;187(19):6824–31.
- Vilei EM, Abdo EM, Nicolet J, Botelho A, Goncalves R, Frey J. Genomic and antigenic differences between the European and African/Australian clusters of *Mycoplasma mycoides* subsp mycoides SC. Microbiology. 2000;146:477–86.
- Madsen ML, Puttamreddy S, Thacker EL, Carruthers MD, Minion FC. Transcriptome changes in *Mycoplasma hyopneumoniae* during infection. Infect Immun. 2008;76(2):658–63.
- Madsen ML, Nettleton D, Thacker EL, Minion FC. Transcriptional profiling of *Mycoplasma hyopneumoniae* during iron depletion using microarrays. Microbiology. 2006;152:937–44.
- Kordafshari S, Marenda MS, O'Rourke D, Shil P, Noormohammadi AH. Mutation of *oppF* gene in the *Mycoplasma synoviae* MS-H vaccine strain and its implication for differential serological responses to vaccination versus field challenge. Vet Microbiol. 2019;231:48–55.
- Lopez CS, Alice AF, Heras H, Rivas EA, Sanchez-Rivas C. Role of anionic phospholipids in the adaptation of *Bacillus subtilis* to high salinity. Microbiology. 2006;152:605–16.
- Serre L, de Jesus KP, Zelwer C, Bureaud N, Schoentgen F, Benedetti H. Crystal structures of YBHB and YBCL from *Escherichia coli*, two bacterial homologues to a Raf kinase inhibitor protein. J Mol Biol. 2001;310(3):617–34.

27. Av-Gay Y, Everett M. The eukaryotic-like Ser/Thr protein kinases of *Mycobacterium tuberculosis*. *Trends Microbiol.* 2000;8(5):238–44.
28. Bakal CJ, Davies JE. No longer an exclusive club: eukaryotic signalling domains in bacteria. *Trends Cell Biol.* 2000;10(1):32–7.
29. Wang JY, Li CH, Yang CJ, Mushegian A, Jin SG. A novel serine/threonine protein kinase homologue of *Pseudomonas aeruginosa* is specifically inducible within the host infection site and is required for full virulence in neutropenic mice. *J Bacteriol.* 1998;180(24):6764–8.
30. Shil PK, Kanci A, Browning GF, Marenda MS, Noormohammadi AH, Markham PF. GapA(+) *Mycoplasma gallisepticum* ts-11 has improved vaccine characteristics. *Microbiology.* 2011;157:1740–9.
31. Goh MS, Gorton TS, Forsyth MH, Troy KE, Geary SJ. Molecular and biochemical analysis of a 105 kDa *Mycoplasma gallisepticum* cytoadhesin (GapA). *Microbiology.* 1998;144:2971–8.
32. Papazisi L, Troy KE, Gorton TS, Liao X, Geary SJ. Analysis of cytoadherence-deficient, GapA-negative *Mycoplasma gallisepticum* strain R. *Infect Immun.* 2000;68(12):6643–9.
33. Whithear KG. Avian Mycoplasmosis. In: Bagust TJ, Corner LA, editors. Australian standard diagnostic techniques for animal diseases. Melbourne: CSIRO for the standing committee on agriculture and resource management; 1993. p. 1–12.
34. Darling AE, Mau B, Blattner FR, Perna NT. GRIL: genome rearrangement and inversion locator. *Bioinformatics.* 2004;20(1):122–4.
35. Rissman AI, Mau B, Biehl BS, Darling AE, Glasner JD, Perna NT. Reordering contigs of draft genomes using the mauve aligner. *Bioinformatics.* 2009;25(16):2071–3.
36. Bertels F, Silander OK, Pachkov M, Rainey PB, van Nimwegen E. Automated reconstruction of whole-genome phylogenies from short-sequence reads. *Mol Biol Evol.* 2014;31(5):1077–88.
37. Tamura K, Stecher G, Peterson D, Filipski A, Kumar S. MEGA6: Molecular evolutionary genetics analysis version 6.0. *Mol Biol Evol.* 2013;30(12):2725–9.
38. Kelley LA, Mezulis S, Yates CM, Wass MN, Sternberg MJE. The Phyre2 web portal for protein modeling, prediction and analysis. *Nat Protoc.* 2015;10(6):845–58.
39. Wass MN, Kelley LA, Sternberg MJE. 3DLigandSite: predicting ligand-binding sites using similar structures. *Nucleic Acids Res.* 2010;38:W469–73.

Publisher's Note

Springer Nature remains neutral with regard to jurisdictional claims in published maps and institutional affiliations.

Ready to submit your research? Choose BMC and benefit from:

- fast, convenient online submission
- thorough peer review by experienced researchers in your field
- rapid publication on acceptance
- support for research data, including large and complex data types
- gold Open Access which fosters wider collaboration and increased citations
- maximum visibility for your research: over 100M website views per year

At BMC, research is always in progress.

Learn more biomedcentral.com/submissions

